Moving Target Detection in Spatially Heterogeneous Clutter Using Distributed MIMO Radar

Aboulnasr Hassanien*, Braham Himed†, Justin Metcalf†, Brian D. Rigling*

*Department of Electrical Engineering, Wright State University, Dayton, OH 45435, USA
E-mail: {nasr.hassanien; brian.rigling}@wright.edu
†RF Technology Branch, Air Force Research Lab (AFRL/RYMD), WPAFB, OH 45433, USA

***Abstract*—In this paper, we consider the problem of moving target detection in distributed multiple-input multiple-output (MIMO) radar under the assumption of non-homogeneous environment. In particular, we assume the spatial heterogeneous clutter, i.e., clutter reflections from different range bins to be independent and the clutter power changes from one cell to another. Even under the same test cell, the clutter components associated with different transmit-receive pairs are dissimilar due to the azimuth-selective back-scattering of the non-homogeneous clutter. A new method for estimating the non-homogeneous clutter for every transmit-receive pair in a distributed MIMO radar is developed. For each transmit-receive path, the non-homogeneous clutter is modeled as a linear combination of appropriately selected basis vectors. The clutter component is adaptively estimated based on maximizing the clutter power and maximally rejecting the power associated with target reflections. A generalized-likelihood ratio test (GLRT) for moving target detection is also developed. Simulations are provided to demonstrate the performance improvement of the proposed GLRT over existing techniques.**

I. Introduction

Distributed sensing technologies and sensor networks enable receiving radio frequency (RF) electromagnetic signals that are either scattered by, or transmitted from, objects of interest [1]. During the last decade, multiple-input multiple-output (MIMO) radar networks have attracted substantial interest [2]–[8]. Active MIMO radar networks employ widely dispersed antennas to transmit and receive orthogonal waveforms. This allows the overall system to view the target simultaneously from several different directions. The problem of target detection in Gaussian noise using distributed MIMO radar networks has been well investigated [9]–[11]. However, in practical scenarios, the target return is usually observed in the background of noise, clutter, interference, and possibly jamming.

The problem of target detection in the presence of homogeneous clutter/interference using distributed MIMO radar networks has been recently investigated (see, e.g., [12], and references therein). The moving target detector reported in [12] is computationally demanding as it requires evaluating a highly non-linear and non-convex function on a multi-dimensional grid using exhaustive search methods. The problem of moving target detection in spatially non-homogeneous clutter environments has been considered in a number of recent papers [13]–[18]. Non-homogeneous clutter arise in practice because multistatic transmit receive configurations usually result in non-stationary clutter across resolution cells [19]. In addition, in distributed MIMO radar networks, the azimuth-selective back-scattering of the clutter may casue the clutter power to vary significantly from one transmit-receive pair to another even for the same range bin [1]. An elegant approach for moving target detection using distributed MIMO radar networks in spatially non-homogeneous clutter environments was introduced in [13] where a simple discrete clutter model was assumed and a generalized likelihood ratio test (GLRT) based detector was developed. In this paper, we develop a moving target detection technique with robustness to highly non-stationary environments. In this respect, we propose a method for adaptive estimation of the clutter component of each transmit-receive path. Then, a GLRT-based technique for moving target detection is developed. The performance of the proposed technique is assessed in terms of probability of target detection and false alarm rates.

The paper is organized as follows. Section II presents the distributed MIMO radar signal model. The non-homogeneous clutter characterization model is given in Sec. III. In Sec. IV, the proposed moving target detector is developed. Simulation results are given in Sec. V, and conclusions are drawn in Sec. VI.

II. Signal Model

Consider a distributed MIMO radar system comprising M_t widely separated cooperative transmit antennas and M_r widely separated receive antennas. Without loss of generality, it is assumed that all transmit and receive elements are mounted on stationary platforms in a two-dimensional space, e.g., x–y plane. The transmit antennas are used to probe a common area of interest using multiple orthogonal waveforms [4], [13], [20]. Each transmit antenna radiates a succession of N periodic pulses over a coherent processing interval (CPI). At each receiver, a bank of M_t matched filters is employed during each radar pulse to extract the signals associated with each transmit-receive path. For each transmit-receive pair, the matched-filtering process is typically performed for a number of range bins. Here, we consider only one range bin and restrict our attention to the corresponding slow-time data, i.e., data sampled at the pulse repetition rate.

For each transmit-receive pair, N slow-time samples are stacked in one column vector. Therefore, the $N\times 1$ signal vector associated with the ij^{th} transmit-receive pair is modeled as

$$\mathbf{x}_{ij} = \mathbf{r}_{ij} + \mathbf{c}_{ij} + \mathbf{z}_{ij}, \quad i = 1, \ldots, M_t,\ j = 1, \ldots, M_r, \quad (1)$$

where $\mathbf{r}_{ij}$ denotes the signal vector associated with the moving target return, $\mathbf{c}_{ij}$ denotes the vector of the clutter return, and $\mathbf{z}_{ij}$ is the additive Gaussian noise vector with zero-mean and covariance $\sigma_z^2\mathbf{I}_N$, and $\mathbf{I}_N$ denotes the $N\times N$ identity matrix. In (1), the target return can be expressed as

$$\mathbf{r}_{ij} = \alpha_{ij}\mathbf{a}(f_{ij}), \quad i = 1, \ldots, M_t,\ j = 1, \ldots, M_r, \quad (2)$$

where α_{ij} denotes the unknown complex amplitude which summarizes the propagation environment through the ij^{th} transmit-receive path, f_{ij} is the Doppler frequency associated with the ij^{th} transmit-receive pair, and $\mathbf{a}(f_{ij})$ is the temporal steering vector.

Consider a hypothetical moving target with velocity $\mathbf{v} \triangleq (v_x, v_y)$, where v_x and v_y are the velocity components along the x- and y-axes, respectively. The corresponding Doppler frequency is defined as [13]

$$f_{ij} = \frac{1}{\lambda}\Big(v_x\big(\cos\theta_i + \cos\phi_j\big) + v_y\big(\sin\theta_i + \sin\phi_j\big)\Big), \quad (3)$$

where θ_i and ϕ_j denote the spatial angles of the i^{th} and j^{th} transmit and receive elements with respect to the positive x-axis, respectively, and λ is the wavelength of the carrier. In (2), the $N\times 1$ temporal steering vector is defined as

$$\mathbf{a}(f_{ij}) = \left[1, e^{-\jmath 2\pi F_{ij}}, \ldots, e^{-\jmath 2\pi F_{ij}(N-1)}\right]^T, \quad (4)$$

where $\jmath \triangleq \sqrt{-1}$ and $F_{ij} \triangleq f_{ij}T_{\text{p}}$ is the normalized Doppler frequency and T_{p} denotes the pulse repetition interval (PRI).

A. Problem Statement

The $N\times 1$ signal vector (1) can be rewritten as

$$\mathbf{x}_{ij} = \alpha_{ij}\mathbf{a}(f_{ij}) + \boldsymbol{\chi}_{ij}, \quad i = 1, \ldots, M_t; j = 1, \ldots, M_r, \quad (5)$$

where $\boldsymbol{\chi}_{ij} \triangleq \mathbf{c}_{ij} + \mathbf{z}_{ij}$ is the expected return in the absence of a target of interest, i.e., the return consists of interference plus noise. The problem of interest can be stated as follows. Given the $N\times 1$ observation vectors $\mathbf{x}_{ij},\ i = 1, \ldots, M_t,\ j = 1, \ldots, M_r$, the objective is to detect the absence/presence of a moving target in a certain test cell, i.e., a target with a hypothetical velocity $\mathbf{v}$. This can be stated by the hypothesis test:

$$H_0 : \mathbf{x}_{ij} = \boldsymbol{\chi}_{ij}, \quad (6)$$
$$H_1 : \mathbf{x}_{ij} = \alpha_{ij}\mathbf{a}(f_{ij}) + \boldsymbol{\chi}_{ij}, \quad (7)$$

where hypothesis H_0 corresponds to the absense of target while hypothesis H_1 means the target is present. Our goal is to develop a robust technique to solve the hypothesis testing problem (6)–(7) without the use of seconday data (in range).

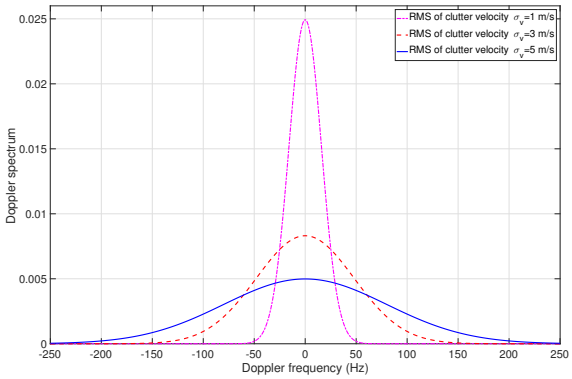

Fig. 1. Clutter PSD for different transmit-receive pairs with different clutter internal velocities.

III. Clutter Characterization

The clutter term $\mathbf{c}_{ij}$ summarizes reflections due to stationary objects such as buildings and slow moving targets such as grass and forest. Therefore, the clutter occupies the low frequency band of the Doppler spectrum. We assume that, for every transmit-receive path, the clutter is characterized by its Doppler power spectral density (PSD) [1], [13]

$$S_{ij}(f_D) = \frac{P_{ij}\lambda}{2\sqrt{2\pi}\sigma_{v;ij}} e^{-\frac{f_D^2\lambda^2}{8\sigma_v^2}}, \quad (8)$$

where f_D is the Doppler frequency variable, P_{ij} is the clutter power, and $\sigma_{v;ij}$ is the root mean-square (RMS) of the clutter internal velocity. It is worth noting that the Doppler PSD S_{ij} is different for different transmit-receive paths due to the non-homogeneous environment. Figure 1 shows the PSD of the clutter as a function of the Doppler frequency in several cases of the RMS of the clutter internal velocity when the clutter power is unity. The figure demonstrates that the PSD of the clutter is in general located in the low frequency region, and the clutter spread is controlled by $\sigma_{v;ij}$. It is observed from the figure that the smaller the value of $\sigma_{v;ij}$, the more spiked the clutter PSD. In other words, the spread of the clutter PSD is narrow when the RMS of the clutter internal velocity is small. As the RMS of the clutter internal velocity increases, the spread of the clutter PSD becomes broader.

Computing the inverse Fourier transform of the clutter PSD (8), the temporal correlation function of the clutter associated with the ij^{th} transmit-receive path can be obtained as [1]

$$r_{ij}(\tau) = \int_{-\infty}^{\infty} S_{ij}(f_D)e^{\jmath 2\pi f_D\tau} df_D$$
$$= P_{ij}e^{-8\left(\frac{\pi\tau\sigma_{v;ij}}{\lambda}\right)^2}. \quad (9)$$

The discrete correlation function of the clutter is obtained by sampling the temporal correlation function (9) at $\tau = nT_p$,

that is, $\tilde{r}(n) \triangleq r(nT_p),\ n = 0, 1, \ldots, N-1$. Therefore, the covariance matrix of the clutter is obtained as

$$\mathbf{C}_{ij} = \begin{pmatrix} \tilde{r}_{ij}(0) & \tilde{r}_{ij}(1) & \ldots & \tilde{r}_{ij}(N-1) \\ \tilde{r}_{ij}(1) & r_{ij}(0) & \ldots & \vdots \\ \vdots & \vdots & \ddots & \tilde{r}_{ij}(1) \\ \tilde{r}_{ij}(N-1) & \ldots & \tilde{r}_{ij}(1) & \tilde{r}_{ij}(0) \end{pmatrix}. \quad (10)$$

Alternatively, the clutter covariance matrix can be computed using the approximate formula

$$\mathbf{C}_{ij} = \int_{-\frac{F_s}{2}}^{\frac{F_s}{2}} S_{ij}(f_D)\mathbf{a}(f_D)\mathbf{a}^H(f_D)df_D, \quad (11)$$

where $F_s \triangleq 1/T_p$ is the slow-time sampling frequency. Let $\mu_{ij;n},\ n = 1, \ldots, N$ be the eigenvalues of the positive semi-definite matrix $\mathbf{C}_{ij}$, where $\mu_{ij;1} \geq \mu_{ij;2} \geq \ldots \geq \mu_{ij,N}$. Then, the matrix $\mathbf{C}_{ij}$ can be written as

$$\begin{aligned} \mathbf{C}_{ij} &= \mathbf{U}_{ij}\mathbf{\Lambda}_{ij}\mathbf{U}_{ij}^H + \mathbf{V}_{ij}\mathbf{\Gamma}_{ij}\mathbf{V}_{ij}^H \\ &\approx \mathbf{U}_{ij}\mathbf{\Lambda}_{ij}\mathbf{U}_{ij}^H, \end{aligned} \quad (12)$$

where $\mathbf{\Lambda}_{ij}$ is the $L_{ij} \times L_{ij}$ diagonal matrix which contains the principal eigenvalues of $\mathbf{C}_{ij}$ and $\mathbf{U}_{ij}$ is the $N \times L_{ij}$ matrix which contains the corresponding eigenvectors. In (12), $\mathbf{\Gamma}_{ij}$ denotes the $(N-L_{ij}) \times (N-L_{ij})$ diagonal matrix which contains the non-principal eigenvalues of $\mathbf{C}_{ij}$, i.e., the eigenvalues of approximately zero value. The corresponding eigenvectors are contained in the matrix $\mathbf{V}_{ij}$. For each transmit-receive pair, the number of principal eigenvalues L_{ij} can be selected such that the ratio of the sum of the principal eigenvalues to the sum of all eigenvalues exceeds a certain level, e.g., 99%. This means that the approximation in (12) retains 99% of the clutter energy.

Using (12), we propose to model the clutter signal component in (1) as a linear combination of the principal eigenvectors of $\mathbf{C}_{ij}$, that is,

$$\mathbf{c}_{ij} = \sum_{\ell=1}^{L_{ij}} g_{ij;\ell}\mathbf{u}_{ij;\ell} = \mathbf{U}_{ij}\mathbf{g}_{ij}, \quad (13)$$

where $\mathbf{u}_{ij;\ell}$ is the ℓ^{th} eigenvector, $g_{ij;\ell}$ is the complex weight associated with the ℓ^{th} eigenvector, $\mathbf{g}_{ij} \triangleq [g_{ij;1}, \ldots, g_{ij;L_{ij}}]^T$, and $\mathbf{U}_{ij} \triangleq [\mathbf{u}_{ij;1}, \ldots, \mathbf{u}_{ij;L_{ij}}]$.

IV. Generalized Likelihood Ratio Test

A. Previous Detector

A discrete clutter model was adopted in [13] based on the asummption that the clutter return is caused by a finite number of discrete scatterers. The corresponding clutter signal is modeled as [13]

$$\mathbf{c}_{ij} = \sum_{\ell=1}^{L} \beta_{ij;\ell}\mathbf{a}(f_\ell) = \mathbf{H}\boldsymbol{\beta}_{ij}, \quad (14)$$

where L is the number of discrete clutter components in the Doppler domain, $\beta_{ij;\ell}$ is the unknown coefficient associated with the ℓ^{th} discrete clutter component, $\boldsymbol{\beta}_{ij} = [\beta_{ij;1}, \ldots, \beta_{ij;L}]^T$, $\mathbf{H} \triangleq [\mathbf{a}(f_1), \ldots, \mathbf{a}(f_L)]$, and $\{f_\ell\}_{\ell=1}^L$ are the Doppler frequencies in the low frequency region. Using the GLRT concept, the moving target detector reported in [13] is stated as

$$T_{\text{GLRT}} = \sum_{i=1}^{M_t}\sum_{j=1}^{M_r} \frac{\left|\mathbf{a}^H(f_{ij})\mathbf{P}_{\mathbf{H}}^{\perp}\mathbf{x}_{ij}\right|^2}{\mathbf{a}^H(f_{ij})\mathbf{P}_{\mathbf{H}}^{\perp}\mathbf{a}(f_{ij})} \underset{\mathcal{H}_0}{\overset{\mathcal{H}_1}{\gtrless}} \kappa_D, \quad (15)$$

where κ_D is a threshold properly selected for a given probability of false alarm, and

$$\mathbf{P}_{\mathbf{H}}^{\perp} = \mathbf{I}_N - \mathbf{H}(\mathbf{H}^H\mathbf{H})^{-1}\mathbf{H}^H. \quad (16)$$

B. Proposed Moving Target Detector

Using the signal model (1) and the proposed cluttter model (13), the likelihood function under hypothesis H_1 can be written as

$$\begin{aligned} f_1(\mathbf{X}, \boldsymbol{\alpha}, \mathbf{G}, \sigma_z^2) = \zeta \exp\Big(-\frac{1}{\sigma_z^2}\sum_{i,j} ||\mathbf{x}_{ij} \\ - \alpha_{ij}\mathbf{a}(f_{ij}) - \mathbf{U}_{ij}\mathbf{g}_{ij}||^2\Big), \end{aligned} \quad (17)$$

where $\mathbf{X} = [\mathbf{x}_{11}, \ldots, \mathbf{x}_{M_tM_r}]$ is the $N \times M_tM_r$ data matrix, $\mathbf{G} = [\mathbf{g}_{11}, \ldots, \mathbf{g}_{M_tM_r}]$ is the $L \times M_tM_r$ unknown weight matrix, $\boldsymbol{\alpha} \triangleq [\alpha_{11}, \ldots, \alpha_{M_tM_r}]^T$ is the $M_tM_r \times 1$ vector of reflection coefficients, and $\zeta \triangleq \frac{1}{(\pi\sigma_z^2)^{NM_tM_r}}$. Similarly, the likelihood function under hypothesis H_0 can be written as

$$f_0(\mathbf{X}, \mathbf{G}, \sigma_z^2) = \zeta \exp\Big(-\frac{1}{\sigma_z^2}\sum_{i,j} ||\mathbf{x}_{ij} - \mathbf{U}_{ij}\mathbf{g}_{ij}||^2\Big), \quad (18)$$

The generalized-likelihood ratio testing (GLRT) is based on evaluating the test statistic

$$\text{GLRT} = \frac{\max_{\boldsymbol{\alpha},\mathbf{G},\sigma_z^2} f_1(\mathbf{X}, \boldsymbol{\alpha}, \mathbf{G}, \sigma_z^2)}{\max_{\mathbf{G},\sigma_z^2} f_0(\mathbf{X}, \mathbf{G}, \sigma_z^2)}. \quad (19)$$

The optimization of (19) can be performed by taking the log-likelihood function of the numerator and denominator and optimizing over the unknown parameters $\boldsymbol{\alpha}$, $\mathbf{G}$, and σ_z^2. The derivation is straightforward and similar to the one given in [13]. The detailed proof under the proposed clutter model will be given in a future paper. The proposed moving target detector can thus be stated as

$$T_D = \sum_{i=1}^{M_t}\sum_{j=1}^{M_r} \frac{\left|\mathbf{a}^H(f_{ij})\mathbf{P}_{\mathbf{U}_{ij}}^{\perp}\mathbf{x}_{ij}\right|^2}{\mathbf{a}^H(f_{ij})\mathbf{P}_{\mathbf{U}_{ij}}^{\perp}\mathbf{a}(f_{ij})} \underset{\mathcal{H}_0}{\overset{\mathcal{H}_1}{\gtrless}} \kappa_D, \quad (20)$$

where κ_D is a threshold that can be properly selected for a given probability of false alarm, and

$$\begin{aligned} \mathbf{P}_{\mathbf{U}_{ij}}^{\perp} &\triangleq \mathbf{I}_N - \mathbf{U}_{ij}(\mathbf{U}_{ij}^H\mathbf{U}_{ij})^{-1}\mathbf{U}_{ij}^H \\ &= \mathbf{I}_N - \mathbf{U}_{ij}\mathbf{U}_{ij}^H \end{aligned} \quad (21)$$

is the projection matrix projecting onto the orthogonal complement to the subspace spanned by the clutter basis vector $\mathbf{u}_{ij;\ell},\ \ell = 1, \ldots, L_{ij}$.

C. SINR Loss

To highlight the difference between the proposed moving target detector and the detector developed in [13], we investigate the effect of performing orthogonal projection on the received data before applying target detection. In particular, we analyze the signal-to-interference plus noise ratio (SINR) loss that the method of [13] suffers due to applying the orthogonal projection $\mathbf{P}_{\mathbf{H}}^{\perp}\mathbf{x}_{ij}$ in (15). The SINR in this case is defined as

$$\mathrm{SINR}_1(f_D) = \frac{\sigma_\alpha^2 N^2 \left|\mathbf{a}^H(f_D)\mathbf{P}_{\mathbf{H}}^{\perp}\mathbf{a}(f_D)\right|^2}{\mathbf{a}^H(f_D)\mathbf{P}_{\mathbf{H}}^{\perp}\mathbf{R}_{C+N}\mathbf{P}_{H}^{\perp}\mathbf{a}(f_D)}, \qquad (22)$$

where σ_α is the variance of the target reflection coefficient and $\mathbf{R}_{C+N}$ is the covariance matrix of the interference-plus-noise, that is,

$$\mathbf{R}_{C+N} = \mathrm{E}\{(\boldsymbol{\chi}_{ij} + \mathbf{z}_{ij})(\boldsymbol{\chi}_{ij} + \mathbf{z}_{ij})^H\}. \qquad (23)$$

Similarly, we highlight the SINR loss that the proposed method suffers due to applying the orthogonal projection $\mathbf{P}_{\mathbf{U}_{ij}}^{\perp}\mathbf{x}_{ij}$ in (20). The SINR for the proposed method is defined for each transmit-receive pair as

$$\mathrm{SINR}_2(f_D) = \frac{\sigma_\alpha^2 N^2 \left|\mathbf{a}^H(f_D)\mathbf{P}_{\mathbf{U}_{ij}}^{\perp}\mathbf{a}(f_D)\right|^2}{\mathbf{a}^H(f_D)\mathbf{P}_{\mathbf{U}_{ij}}^{\perp}\mathbf{R}_{C+N}\mathbf{P}_{\mathbf{U}_{ij}}^{\perp}\mathbf{a}(f_D)}. \qquad (24)$$

The optimal SINR is defined for the case where the target return is contaminated by noise only. In this case, it simplifies to the signal-to-noise ratio (SNR), that is,

$$\mathrm{SNR}_{\mathrm{opt}}(f_D) = \frac{\sigma_\alpha^2 N^2}{\mathbf{a}^H(f_D)\sigma_z^2\mathbf{I}_N\mathbf{a}(f_D)} = \frac{\sigma_\alpha^2}{\sigma_z^2}N. \qquad (25)$$

The SINR loss is defined as the ratio of the actual SINR to the optimal SINR.

V. Simulation Results

In our simulations, we assume a distributed MIMO radar system comprising multiple transmit and multiple receive antennas which are widely separated from each other. In the first example, we examine the SINR loss for the proposed method, the discrete Doppler model adopted in [13] as well as for the matched-filter case. The carrier frequency used is 1 GHz and the pulse repetition frequency is 1 kHz, i.e., PRI is 1 ms. In the first example, we assume that $N = 128$ pulses are collected during a CPI. We consider two cases where the clutter internal velocities are $\sigma_v = 1$ m/s and $\sigma_v = 5$ m/s, respectively. Fig. 2 shows the SINR loss for all methods when the clutter-to-noise ratio (CNR) is 30 dB. We assume that an SINR loss of -10 dB or less is acceptable for reliable detection. The figure shows that the proposed method has an SINR loss that is almost the same as that of the matched-filter. This means that the minimum detectable target velocity (i.e., SINR loss at -10 dB) is almost the same for the proposed method and the matched-filter. On the other hand, the minimum detectable velocity for the method of [13] is much larger than the one for the matched-filter. Fig. 3 shows the SINR loss for all methods when the clutter-to-noise ratio

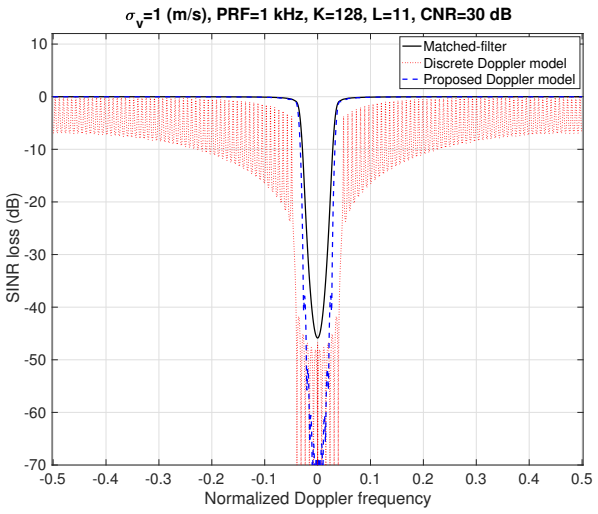

Fig. 2. SINR loss versus normalized Doppler frequency.

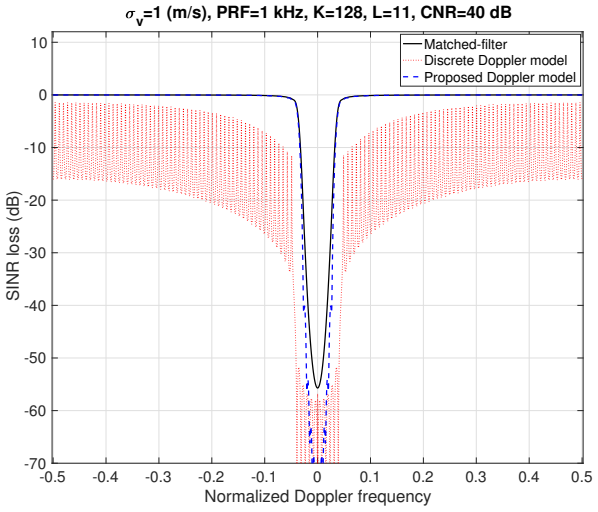

Fig. 3. SINR loss versus normalized Doppler frequency.

(CNR) is 40 dB, i.e., strong clutter return. The figure shows that the proposed method is robust to powerful clutter returns and performs similar to the matched-filter. On the other hand, the method of [13] exhibits a fluctuating performance over the entire Doppler range, i.e., at some Doppler frequencies the SINR loss is higher than -10 dB and at other Doppler frequencies it is lower than -10 dB. Figs 4 and 5 show the SINR loss for all methods tested for the case of $\sigma_v = 5$ m/s, i.e., for the case where the clutter is widely spread in the Doppler domain. The two figures mirror the results shown in Figs. 2 and 3. The figures show that the proposed method is robust to clutter power variation and clutter spread in the Doppler domain.

In the second example, we test the probability of detection versus the probability of false alarm. The carrier frequency used is 1.5 GHz and the pulse repetition frequency is 400 Hz,

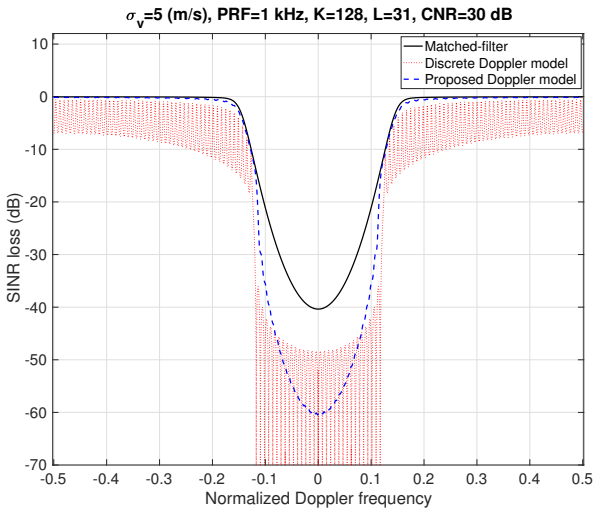

Fig. 4. SINR loss versus normalized Doppler frequency.

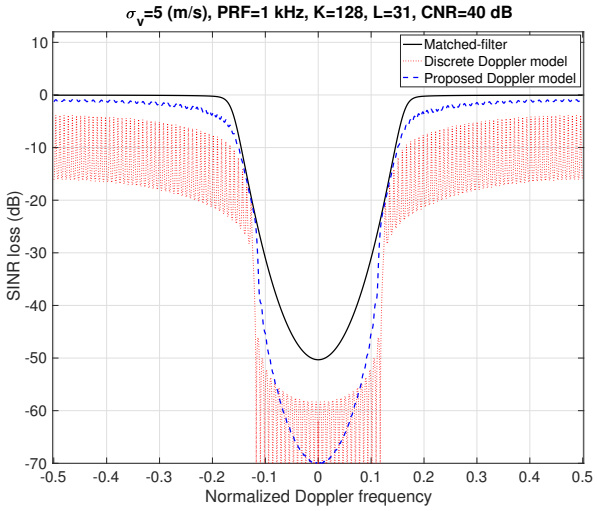

Fig. 5. SINR loss versus normalized Doppler frequency.

i.e., PRI is 2.5 ms. $N = 12$ pulses are collected during a CPI. The performance of the proposed moving target detector (20) is compared to the performance of the detector of [13]. We assume that $M_t = 2$ transmit antennas and $M_r = 2$ receiver antennas are used. The transmit antennas are located at directions $0°$ and $65°$ with respect to the x–axis. The receive antennas are located at directions $-30°$ and $40°$ with respect to the x–axis. The moving target has speed 30 m/s (108 km/h) in the direction $30°$. Fig. 6 shows the probability of detection versus probability of false alarm for a fixed SNR of 15 dB and a fixed CNR of 40 dB. It is clear from the figure that the proposed detector has superior detection performance for all clutter internal velocity values tested.

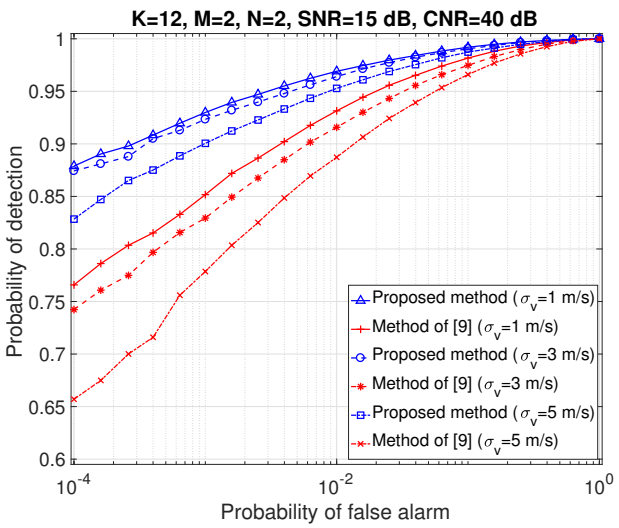

Fig. 6. Probability of detection versus probability of false alarm.

VI. Conclusion

The problem of moving target detection in distributed multiple-input multiple-output (MIMO) radar under the assumption of spatially heterogeneous clutter environment was considered. It is assumed that the clutter power and Doppler spread changes from one cell to another. Even under the same cell, the clutter components associated with different transmit-receive pairs are dissimilar due to the azimuth-selective backscattering of the distributed MIMO radar. A new method for estimating the non-homogeneous clutter for every transmit-receive pair was developed. For each transmit-receive path, the clutter is modeled as a linear combination of appropriately selected basis vectors. The clutter component is adaptively estimated based on maximizing the clutter power and maximally rejecting the power associated with target reflections. A generalized-likelihood ratio test (GLRT) for moving target detection was developed.

References

[1] M. Skolnik, *Introduction to Radar Systems*. McGraw Hill, 3rd edition ed., 2002.

[2] E. Fishler, A. Haimovich, R. Blum, D. Chizhik, L. Cimini, and R. Valenzuela, "Mimo radar: An idea whose time has come," in *IEEE Radar Conference*, pp. 71–78, 2004.

[3] J. Li and P. Stoica, "MIMO radar with colocated antennas," *IEEE Signal Processing Magazine*, vol. 24, no. 5, pp. 106–114, 2007.

[4] A. M. Haimovich, R. S. Blum, and L. J. Cimini, "MIMO radar with widely separated antennas," *IEEE Signal Processing Magazine*, vol. 25, no. 1, pp. 116–129, 2008.

[5] A. Hassanien and S. A. Vorobyov, "Why the phased-MIMO radar outperforms the phased-array and MIMO radars," in *2010 18th European Signal Processing Conference*, pp. 1234–1238, Aug 2010.

[6] Y. Li, S. A. Vorobyov, and A. Hassanien, "MIMO radar capability on powerful jammers suppression," in *2014 IEEE International Conference on Acoustics, Speech and Signal Processing (ICASSP)*, pp. 5277–5281, May 2014.

[7] A. Hassanien, S. A. Vorobyov, and A. Khabbazibasmenj, "Transmit radiation pattern invariance in MIMO radar with application to DOA estimation," *IEEE Signal Processing Letters*, vol. 22, pp. 1609–1613, Oct 2015.

[8] M. Y. Cao, S. A. Vorobyov, and A. Hassanien, "Transmit array interpolation for DOA estimation via tensor decomposition in 2-D MIMO radar," *IEEE Transactions on Signal Processing*, vol. 65, pp. 5225–5239, Oct 2017.

[9] D. E. Hack, L. K. Patton, B. Himed, and M. A. Saville, "Centralized passive MIMO radar detection without direct-path reference signals," *IEEE Transactions on Signal Processing*, vol. 62, pp. 3013–3023, June 2014.

[10] D. E. Hack, L. K. Patton, B. Himed, and M. A. Saville, "Detection in passive MIMO radar networks," *IEEE Transactions on Signal Processing*, vol. 62, pp. 2999–3012, June 2014.

[11] J. Liu, H. Li, and B. Himed, "Two target detection algorithms for passive multistatic radar," *IEEE Transactions on Signal Processing*, vol. 62, pp. 5930–5939, Nov 2014.

[12] Q. He, N. H. Lehmann, R. S. Blum, and A. M. Haimovich, "MIMO radar moving target detection in homogeneous clutter," *IEEE Transactions on Aerospace and Electronic Systems*, vol. 46, pp. 1290–1301, July 2010.

[13] P. Wang, H. Li, and B. Himed, "Moving target detection using distributed MIMO radar in clutter with nonhomogeneous power," *IEEE Transactions on Signal Processing*, vol. 59, pp. 4809–4820, Oct 2011.

[14] P. Wang, H. Li, and B. Himed, "A parametric moving target detector for distributed MIMO radar in non-homogeneous environment," *IEEE Transactions on Signal Processing*, vol. 61, pp. 2282–2294, May 2013.

[15] T. Boukaba, A. M. Zoubir, and D. Berkani, "Robust parametric detection in non homogeneous clutter," in *Sensor Array and Multichannel Signal Processing Workshop (SAM), 2014 IEEE 8th*, pp. 473–476, IEEE, 2014.

[16] Z. Wang, H. Li, and B. Himed, "A sparsity based GLRT for moving target detection in distributed MIMO radar on moving platforms," in *2015 49th Asilomar Conference on Signals, Systems and Computers*, pp. 90–94, Nov 2015.

[17] A. Mandal and R. Mishra, "Design and performance analysis of LMS algorithm based adaptive filter embedded with CFAR detector under non-homogeneous clutter scenarios," *International Journal of Adaptive Control and Signal Processing*, vol. 30, no. 7, pp. 941–956, 2016.

[18] G. Foglia, C. Hao, A. Farina, G. Giunta, D. Orlando, and C. Hou, "Adaptive detection in partially homogeneous clutter with symmetric spectrum," *IEEE Transactions on Aerospace and Electronic Systems*, 2017.

[19] N. J. Willis and H. D. Griffiths, *Advances in bistatic radar*, vol. 2. SciTech Publishing, 2007.

[20] A. Hassanien, S. A. Vorobyov, and A. B. Gershman, "Moving target parameters estimation in noncoherent MIMO radar systems," *IEEE Transactions on Signal Processing*, vol. 60, pp. 2354–2361, May 2012.